
Full Paper

Investigation of the Corrosion of Aluminum Soft Drink Packaging in A Citric Acid Environment with Catalytic Ions Through the Box-Behnken Design Approach

Sara Lahmady, and Issam Forsal*

Laboratory of Engineering and Applied Technologies, School of Technology, Beni Mellal, Morocco

*Corresponding Author, Tel.: +212661118208

E-Mail: forsaliissam@usms.ma

Received: 5 December 2023 / Accepted with minor revision: 28 January 2024 /

Published online: 31 January 2024

Abstract- The corrosion of aluminum beverage cans poses a significant industrial challenge that causes economic and health problems. However, there exists a requirement to gather scientific data that can offer knowledge to the food and packaging sectors, aiding in enhancing materials and reducing losses linked to this issue. This research examined how aluminum cans interacted with beverages using model solutions containing copper and chloride concentrations close to those typically found in beverages. This research highlights the influence of the temperature (20-50°C), chloride concentration (25-1000 mg/L), and copper concentration (25-1000 µg/L) as independent variables on the corrosion of Al can in citric acid solution using Response surface methodology (RSM) with the Box–Behnken design (BBD). The input corrosion current density was assessed through potentiodynamic polarization tests conducted under variable conditions outlined in the design matrix. With p-values under 0.05 and good regression coefficients (R^2), the (ANOVA) approach confirmed that the quadratic model developed was significant. The RSM demonstrated a strong alignment between the predicted outcomes and the observed responses. The $[Cl^-]$ exhibited the most prominent and adverse impact on the dissolution of aluminum. The EIS graphs indicated that the corrosion reaction is primarily governed by the diffusion process.

Keywords- Aluminum; Corrosion; Box Behnken design; Electrochemical tests; Response surface methodology (RSM)

1. INTRODUCTION

Aluminum is frequently used as metal packaging in various industries particularly in the food and beverage sector due to its exceptional properties and versatility such as the combination of strength, lightness, recyclability and formability [1,2]. Aluminum packaging provides effective protection for products, safeguarding them from external elements like moisture and light. This preservation ensures items quality and extends their shelf life [3,4].

Based on the available literature, aluminum beverage packaging is commonly found in the form of cans and bottles, both crafted from two different aluminum alloys. The body of the can (bottom and wall) is typically constructed using the 3104 alloy, this specific choice is attributed to the alloy's ductility, enabling the walls to be efficiently stretched and ironed during the can-forming process [1,5]. The 5182 alloy is employed for the can's top (closure) due to its commendable corrosion resistance, however, unlike the 3104 alloy, it lacks ductility, mainly due to its higher magnesium content in the composition [1,6].

Aluminum is acknowledged for its innate corrosion protection, which arises from the development of a thin oxide layer on its surface [7]. Nevertheless, various factors can contribute to corrosion in beverage packaging, including the acidity of certain beverages, notably fruit juices and soft drinks with low pH values (often $\text{pH} < 4.5$), the presence of oxygen as well as the dissolved ions, temperature fluctuation and mechanical damage [8,9]. In a previous investigation conducted by Danillo S. Soares et al in 2017, the influence of catalytic ions, such as iron and chloride in an acidic medium, on the corrosion of aluminum packaging (specifically AA3104-H19 alloy) was studied using polarization curves [1]. Additionally, in another study, the authors demonstrated that the corrosion process can be sped up when copper and chloride ions are present in the beverage or come into contact with the Al surface [10]. The issue of internal corrosion leads to a degradation in product quality and purity, as well as the transfer of aluminum into beverages, leading to health issues and financial consequences for the food industry [11]. The migration of metals from the package to the food can render it unfit for consumption if the concentration of metal is higher than the tolerated limits [8]. High levels of aluminum in food may lead to the neurological disorders such as Alzheimer's disease and Parkinson's disease [12,13]. However, various regulatory authorities and organizations have established guidelines and limits for acceptable levels of aluminum in these products to ensure consumer safety. The European Food Safety Authority (EFSA) has established a tolerable weekly intake (TWI) of 1 milligram of aluminum per kilogram of body weight per week [14].

Despite the risk associated with this problem, there is a lack of information on corrosion of aluminum food packaging in the literature, particularly concerning corrosion catalysts present in food and drinks. Hence, it holds great importance to investigate the interaction of this packaging with beverages to gain a deeper understanding of the underlying processes involved. For this reason, the main aim of this research is to explore the impact of three independent variables, namely chloride ions, copper ions, and temperature, on the corrosion of aluminum

used in drinks cans within an acidic solution (citric acid). In this investigation a mathematical and statistical methods, specifically response surface methodology (RSM) and Box-Behnken design (BBD), were employed to analyse and quantify the relationships between these variables and the corrosion process.

A traditional experimental investigation cannot adequately characterize the behavior of the metal/solution interface since the corrosion mechanism depends on different factors. To overcome this limitation, our study integrates experimental and statistical method in an effort to improve our comprehension of corrosion attenuation. To build a statistical model that could describe aluminum corrosion under various circumstances and optimize the influence of selected independent variables, we used the design of experiment (DoE) technique. Our findings were verified by the analysis of variance (ANOVA). A variety of electrochemical techniques were employed to examine the corrosion of this particular type of aluminum, including Potentiodynamic Polarization (PDP) and Electrochemical Impedance Spectroscopy (EIS). Scanning Electron Microscopy (SEM) was used to evaluate the surface characteristics to validate the effect of the independent factors considered.

2. MATERIALS AND METHODS

2.1. Preparation of metal specimens

In this investigation, a sheet of aluminum cans, obtained from a standard batch commercialised in the Moroccan market, was used. Consequently, the analysis was conducted with a real and representative sample. The body wall of the aluminum can was employed for all of the specimens used in the current investigation. The top and bottom pieces of the can were taken out, and the wall was unravelled to eliminate any potential effects from the ironing procedure, which is involved in the can's construction. All used packages were collected from new packages and did not contain any physical damage. Before each electrochemical experiment, all samples were prepared by removing the varnish and the inner coating with a solvent, followed by polishing them with emery paper (from 600 to 1200) and rinsing them with distilled water, degreased with acetone, and dried with warm air. It should be mentioned that the working electrode's exposed area is 0.6 cm^2 .

2.2. Model solutions

We used the model solutions in the execution of this study to gain a better and deeper understanding of the corrosion problems of Al beverage cans. By employing this approach, it is possible to regulate the ingredients and qualities of the products. Additionally, this strategy enables the repetition of trials with reliable outcomes. The preparation of solutions was guided by earlier research involving multiple beverages, which aimed to simulate the real products using simplified formulation. To produce a solution with a pH level of 3, similar to some

beverages packed in aluminum cans [10], each model solution was created by mixing distilled water with citric acid monohydrate $C_6H_8O_7 \cdot H_2O$ (Merck). Different concentrations of the copper ions from $CuSO_4 \cdot 5H_2O$ (Merck) and chloride ions derived from $NaCl$ (Merck) were incorporated to obtain the required solutions for this investigation.

2.3. Design of Experiment (DoE) and Response Surface Methodology (RSM)

The conventional methods examine just one variable over time while maintaining the other variables constant, making it impossible to analyse the interaction between two or more variables; One Factor at a Time (OFAT) [15,16]. Nevertheless, these classical approaches are expensive [17], requiring a lot of testing, as well as time and work. Design of experimental (DoE) is an excellent method for demonstrating the impact of numerous independent variables, especially when complex relationships are present [18].

A statistical Design of Experiment (DoE) is a method for collecting data, creating an empirical model to reduce the number of tests, and determining significant variables and interactions that impact the process response [19]. Usually, it is carried out using techniques like full factorial design, fractional factorial design and Response surface design (RSM) [20]. The most informative method is (RSM), it encompasses a set of statistical techniques (DOE) that uses mathematical and statistical methods for modelling, evaluating, and optimizing complicated situations [21,22]. In addition, Response surface methodology offers graphical representations to demonstrate the link between various experimental factors and the measured value (response) [23].

As we already mentioned, RSM uses a particular mathematical model to suit the data collected by the DoE. This mathematical model encapsulates the relationship between variables or parameters as inputs and responses as outputs [22]. It is better to use a second-order polynomial regression model, as shown in Equation (1), to properly illustrate linear interactions and quadratic impact [24,25]:

$$Y = a_0 + \sum_{i=1}^n a_i X_i + \sum_{i=1}^n a_{ii} X_i^2 + \sum_{i=1}^{n-1} \sum_{j=i+1}^n a_{ij} X_i X_j + \varepsilon \quad (1)$$

where Y: the Response or the dependent parameter; a_0 symbolizes the constant term of the model; a_i , a_{ii} , and a_{ij} denote the regression coefficients of linear, square, and interaction terms of the mode, respectively; X_i and X_j are the independent variables.; while ε stands for the stochastic or random error.

Many designs may be utilized in response surface methodology, the diversity between these designs is based on the number of factors and levels considered, as well as the selection of experimental points. For fitting a second-order model in RSM, Central Composite Design (CCD) and Box-Behnken Design (BBD) are two very useful and popular methods [19].

2.4. box Behnken design (BBD) and Design Matrix

The Box-Behnken design (BBD) at three levels was chosen for this study with the intention of revealing the relationship between response functions and factors. Compared to CCD and other options, the BBD, created by Box and Behnken in 1960, is a significantly more efficient design [26-28]. The benefit of BBD is that it eliminates trials conducted in extreme circumstances since it has no axial points, ensuring that all points lie within the safe operating zone, also it only requires a relatively small group of factors to determine the complicated response function [22].

The levels of the factors in the Box-Behnken design are positioned in the center of the cubical design space as well as at the midpoints of its edges (Figure 1). A three-factor design is demonstrated in the following figure [29]:

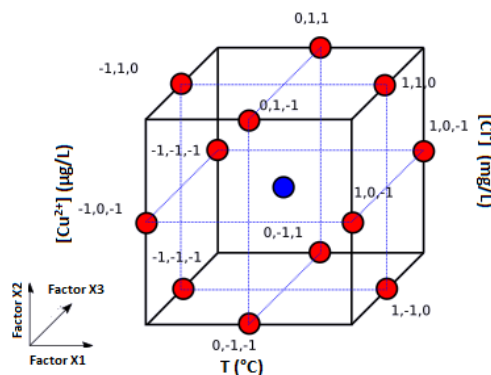


Figure 1. BBD Cube plot

In this investigation, three parameters (temperature, copper concentration and chloride concentration) were employed, and the examined interval of these independent factors was determined in accordance with the literature [22]. Each factor has levels (minimum, medium, maximum) which are coded as (-1, 0, and +1). Table 1 includes real and coded values for the chosen range of variables that affect corrosion of aluminum beverage cans. The response (I_{corr}) was related to the selected variables by the second-order polynomial regression model given in Equation (1).

Table 1. Parameters with their associated uncoded values and their corresponding coded levels

Variable	Code value		
	-1 (Minimum)	0 (Medium)	1 (Maximum)
X ₁ , Temperature T (°C)	20	35	50
X ₂ , Copper concentration [Cu ²⁺] (µg/L)	25	512.5	1000
X ₃ , Chloride concentration [Cl ⁻] (mg/L)	25	512.5	1000

Using the Design Expert software, the design of experiment was executed according to the testing range. An experiment number of $N = 2k(k-1) + cp$, where k is the number of variables and cp is the number of trials at the center point, was necessary for the RSM utilizing the Box-Behnken design [30]. Utilizing duplicates and adding a small number of center points are two strategies to get sufficient data. Since repetition could take time, this design incorporates three experiments conducted precisely at the central point [19]. Since there are three center points (cp) and three components (k) in this inquiry, there were a total of 15 trials, as shown in the Table 2 below.

Table 2. The experimental design for the test elements using Box Behnken design matrix

		Real variable			Coded variable		
Std Order	Run Order	T (°C)	[Cu ²⁺] (µg/L)	[Cl ⁻] (mg/L)	X ₁	X ₂	X ₃
4	1	50	1000.0	512.5	1	1	0
9	2	35	25.0	25.0	0	-1	-1
2	3	50	25.0	512.5	1	-1	0
13	4	35	512.5	512.5	0	0	0
11	5	35	25.0	1000.0	0	-1	1
12	6	35	1000.0	1000.0	0	1	1
6	7	50	512.5	25.0	1	0	-1
14	8	35	512.5	512.5	0	0	0
10	9	35	1000.0	25.0	0	1	-1
3	10	20	1000.0	512.5	-1	1	0
7	11	20	512.5	1000.0	-1	0	1
15	12	35	512.5	512.5	0	0	0
5	13	20	512.5	25.0	-1	0	-1
8	14	50	512.5	1000.0	1	0	1
1	15	20	25.0	512.5	-1	-1	0

2.5. Performing Electrochemical Experiments

Every electrochemical test was carried out using a potentiostat OrigaStat 100 controlled via the Origamaster5 program. The usual three-compartment electrochemical cell was employed, with a platinum as the auxiliary electrode, a saturated calomel electrode (SCE) as the reference electrode, and aluminum as the working electrode. Before measurements, the aluminum electrode was submerged for an hour in the corrosive solutions to have a stable state of open circuit potential (E_{ocp}). Potentiodynamic polarization curves were obtained in the potential range of -1100 to 400 mV compared to the (SCE) reference electrode, from cathodic to anodic orientation, at a scan rate of 1 mV.s⁻¹. Electrochemical impedance was measured at open circuit

potential (E_{OCP}) at frequencies between 100 mHz and 1 kHz. Signals with sine wave voltages of 0.01 V peak to peak were applied. The EC-Lab program was used to fit the results.

2.6. Scanning electron microscopy analysis

Scanning electron microscopy (SEM) was employed as a potent analytical method to comprehend the surface morphology of the investigated aluminum can sample. We performed this analysis before and after immersion of the aluminum in a simulated solution of real soft drinks for durations of 6 and 24 hours. The type of (SEM) instrument is JSM-IT10.

3. RESULTS AND DISCUSSION

3.1. PDP results according the box Behnken design matrix

To examine the influence of the three chosen factors on the corrosion behavior of aluminum cans, polarization measurements were performed in accordance with the abovementioned BBD matrix. Following the OCP measurements, the PDP of working electrode was measured from the hydrogen evolution area (-1.4 V) to the anodic potential zone (0.4 V). The corrosion current density (I_{corr}) for the RSM with BBD was calculated using the PDP curves. Figure 2 displays the PDP curves for aluminum after 1 hour of immersion in a citric acid solution (pH 3) containing varied concentrations of copper and chloride ions at various temperatures.

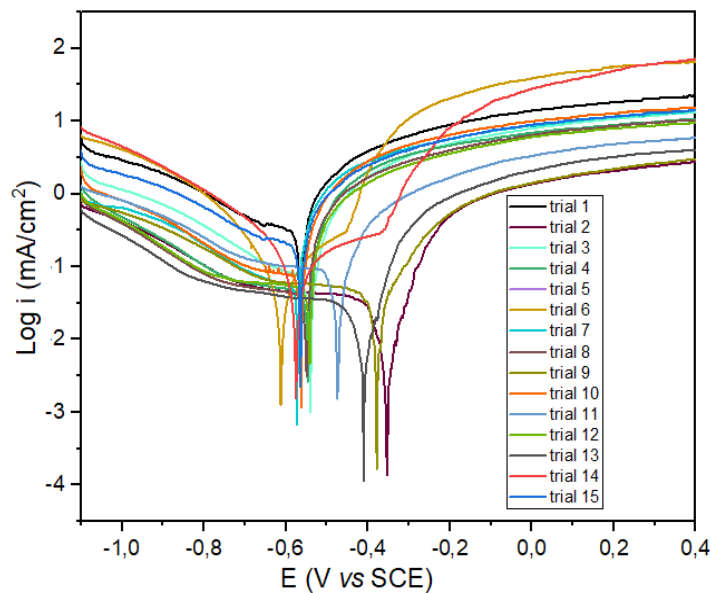
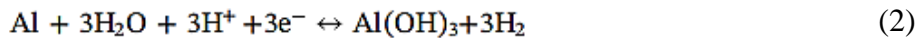


Figure 2. PDP curves of Al electrode according the experimental design of RSM with Box Behnken Design

According to the entirety electrochemical process (Equation 2), the consequences were caused by the aluminum's fast dissolution and the creation of aluminum hydroxide [31].



The gained plots demonstrate that the three parameters (T , $[\text{Cu}^{2+}]$ and $[\text{Cl}^-]$) under consideration exert an influence on the form of the polarization curves within the citric acid environment. The profile of the curves substantiates the impact of various tested variables on the performance of working electrode, suggesting that they contribute to the degradation of the oxide film formed on aluminum during anodic polarization in citric acid.

The current density (I_{corr}) rises with temperature and increases with chloride and copper ion concentrations, according to analysis of the polarization curves. It is observed that the three factors have an impact on both the cathodic and anodic Tafel lines. As depicted in the figure 2, when the concentrations of ions (copper and chloride) and temperature decrease, the values of E_{corr} are slightly shifted towards the positive direction.

In this study, it was found that no additional passive film developed during the anodic polarization of aluminum when it was operated in a citric acid environment with a pH of 3 with the presence of copper and chloride ions. A comparable pattern was noted in acetic acid with a pH of 2 [32]. This behavior was elucidated by SERUGA et al, suggesting that the potent dissolution of the initial oxide layer, and the film-degrading impact likely caused by the elevated concentration of H^+ ions, prevents the formation of a protective passive film during anodization. This breakdown of passivity can potentially result in significant metal dissolution or corrosion localized to specific areas [32].

As documented in the literature, aluminum may corrode in solutions containing halogen ions. At any pH, halogen ions increased the corrosion of Al [30]. This happened more quickly in an acidic environment. Chloride ions (Cl^-) have been singled out as the predominant instigators of aluminum corrosion. Due to its small radius, diffusion of Chloride ion proved difficult to obstruct. After the attachment of chloride ion to the aluminum surface, because to its high activity, it interacted with the passivation layer or metal of Al and slowly broke the film to produce small pits [31].

It is well known that the Al surface corrodes when copper ions are present. Copper ions create a galvanic cell that pits aluminum. Bakos et al. substantiated this by revealing that an Al-Cu bimetallic system is produced when aluminum is submerged in a solution containing copper ions due to the deposition of copper ions on the surface of aluminum. Consequently, it can be deduced that the aluminum-copper (Al-Cu) couple becomes galvanically interconnected [33].

3.2. The statistical second-order model

The response of the model (corrosion current density) was calculated using the Tafel extrapolation method. The result of these 15 experimental runs is given in Table 3.

Table 3. Experimental and predicted data for response (I_{corr})

Run Order	Parameters			I_{corr} ($\mu\text{A}/\text{cm}^2$)	
	T (°C)	[Cu ²⁺] ($\mu\text{g}/\text{L}$)	[Cl ⁻] (mg/L)	Experiment	Prediction
1	50	1000.0	512.5	160.30	159.34
2	35	25.0	25.0	30.30	29.71
3	50	25.0	512.5	98.25	95.63
4	35	512.5	512.5	47.55	47.10
5	35	25.0	1000.0	57.45	59.691
6	35	1000.0	1000.0	150.40	150.94
7	50	512.5	25.0	54.90	58.10
8	35	512.5	512.5	45.20	47.10
9	35	1000.0	25.0	39.20	36.96
10	20	1000.0	512.5	74.50	77.12
11	20	512.5	1000.0	65.52	62.32
12	35	512.5	512.5	47.5	47.10
13	20	512.5	25.0	35.25	34.85
14	50	512.5	1000.0	174.23	174.60
15	20	25.0	512.5	41.36	42.32

Upon examining Table 3 and comparing runs 7 and 14, a substantial rise in (I_{corr}) for the procedure following the change in chloride concentration from 25 mg/L to 1000 mg/L under the conditions of an isothermal experimental setup. Nevertheless, in the case of experiments 2 and 9, no notable increase in corrosion current density when copper concentration increased from 25 to 1000 g/L, despite the tests were carried out under constant conditions. On the other hand, the results of tests 7 and 13 demonstrate that increasing temperatures notably accelerates the dissolution of aluminum cans. Referring to the information provided in Table 3, experiment number 2 showed the lowest corrosion current density ($30.3 \mu\text{A}/\text{cm}^2$). This outcome was achieved through the utilization of a moderate temperature (35°C), with the lowest concentrations of chloride (25 mg/L) and copper (25 $\mu\text{g}/\text{L}$). Conversely, experiment number 3 yielded the highest corrosion rate, which was attributed to the combination of elevated chloride concentration (1000 mg/L), higher temperature (50°C), alongside a moderate concentration of copper (512.5 $\mu\text{g}/\text{L}$). The results show that each of the elements under investigation seems to have a negative impact on the response. This implies that increasing these components causes

the increase of corrosion current density. Therefore, accelerating the degradation of aluminum beverage cans.

In order to create mathematical model to represent experimental data, the output variable (response) was linked to the independent variables based on the regression analysis. In this study the corrosion current density was subsequently evaluated by RSM with BBD using Design Expert software with the intent to develop a regression equation of the relationship between the parameters. The model (second-order polynomial) is presented in the equation (3) below in terms of uncoded variables.

$$\begin{aligned} I_{\text{corr}} = & 186.8 - 9.086 T - 0.1013 [\text{Cu}^{2+}] - 0.1019 [\text{Cl}^-] + 0.13254 T^2 + 0.000070 \\ & [\text{Cu}^{2+}]^2 + 0.000023 [\text{Cl}^-]^2 + 0.000988 T * [\text{Cu}^{2+}] + 0.003044 T * \\ & [\text{Cl}^-] + 0.000088 [\text{Cu}^{2+}] * [\text{Cl}^-] \end{aligned} \quad (3)$$

The predicted results shown in Table 3 were produced by using the second order model (Equation 3). This model shed light on the quadratic and interaction effects of the factors on the corrosion current density of aluminum in a simulation of beverages. The techniques used to verify the equation's accuracy will be explained in subsequent parts.

3.3. Analysis of Variance (ANOVA) Test and Fit Statistics

One of the most essential methods in statistical analysis is the analysis of variance (ANOVA) test [34]. It is a helpful tool that assesses the significance of models, individual experimental parameters, and their interactions using P-values and F-values [35]. When a regression model's P-value is less than 0.050 (the significance threshold) and it displays a high F-value, it is deemed to be the best appropriate statistical model for the observed data points. the ANOVA test results and the fit statistics for the corrosion current density mode are illustrated in Tables 4 and 5.

A p-value in statistical analysis indicates the potential of the regression model [11]. The alpha value for this inquiry was 5% since the confidence interval (%CI) was set at 95%. This model's p value is less than 0.05, which demonstrates model validity according to the table ANOVA. There was a considerable difference between the variables as a result. The totality terms' p-values for (I_{corr}) equation regression were below 0.05, which indicated that their addition to the model would likely result in a meaningful impact. Another significant statistical factor that is closely related to the p-value is the F-value. To determine the significance of the mean differences between operating conditions, a F test is performed. Since the F-value for this model is 340.2, which is much higher than the Fcritical value of 4.7725, it may be used to reject the null hypothesis that all of the coefficients are zero [36].

The lack-of-fit test is a statistical concept that is crucial in ANOVA. The chosen model needs to have an important value of lack of fit [34]. When the p-value is larger than 0.10, the

requirement is satisfied. The identified model's lack-of-fit value was 0.10, indicating good fit for the suggested regression model.

Table 4. Variance analysis result for the quadratic regression equation

Source	DF	Sum of Squares	Mean Square	F-Value	P-Value
Model	9	32425.4	3602.8	340.02	< 0.0001
Linear	3	24399.0	8133.0	767.56	< 0.0001
T	1	9184.9	9184.9	866.83	< 0.0001
[Cu ²⁺]	1	4851.1	4851.1	457.83	0.0003
[Cl ⁻]	1	10363.0	10363.0	978.01	0.0003
Square	3	4071.1	1357.0	128.07	< 0.0001
T ²	1	3283.9	3283.9	309.92	< 0.0001
[Cu ²⁺] ²	1	1027.3	1027.3	96.95	< 0.0001
[Cl ⁻] ²	1	113.6	113.6	10.72	0.0022
2-Way Interaction	3	3955.4	1318.5	124.43	0.0001
T*[Cu ²⁺]	1	208.9	208.9	19.72	0.0068
T* [Cl ⁻]	1	1982.0	1982.0	187.06	< 0.0001
[Cu ²⁺] * [Cl ⁻]	1	1764.4	1764.4	166.52	< 0.0001
Error	5	53.0	10.6		
Lack-of-Fit	3	47.1	15.7	5.30	0.1627
Pure Error	2	5.9	3.0		
Total	14	32478.4			

Table 5. Fit statistics of the generated model for corrosion current density (I_{corr})

Statistical Parameter	The model for (I_{corr})
Standard deviation	3.26
Coefficient of variation (%)	4.35
R-Squared	0.9984
Adjusted R ²	0.9954
Predicted R ²	0.9764
Adequate precision	54.515

Important statistical variables like the coefficient of determination (R^2) are listed in Table 5. The agreement of the recommended regression model with the test data points is measured using the R^2 statistic [34,35]. The range of the coefficient of determination is 0 to 1. It is advised to aim for a value close to 1, which represents the best fit of the regression model [34]. The regression equation that was generated has a remarkable high adjusted R^2 value for I_{corr} of 0.9954, demonstrating its robustness.

Another essential fitting statistic is the predicted R^2 , which shows the expected coefficient of determination for the suggested regression model. The corrosion current density's predicted R^2 value stood at 0.9764, whereas the adjusted R^2 value was notably higher at 0.9954, the discrepancy between the predicted R^2 and adjusted R^2 amounted to 0.019. There was an acceptable level of concordance because the variance was in the range of 0.2.

The statistical concept known as "adequate precision" assesses the boundaries of the anticipated error in relation to the estimated output, essentially measuring the signal-to-noise ratio [34]. The examination's current density model has an adequate precision of 37.279. This number is more than 4.0, indicating that the discrimination provided by the model was adequate. Because the outputs of the predicted response are less affected by error, the chosen model expression may be utilized to explore the design regions of the responses.

3.4. Validation of the developed model employing diagnostic plots

Diagnostic tests are necessary in statistics to verify that the conditions for the ANOVA test have been fulfilled and to evaluate the suitability of a built model [36]. One of the helpful graphs for model validation is the predicted versus actual plot (Figure 3).

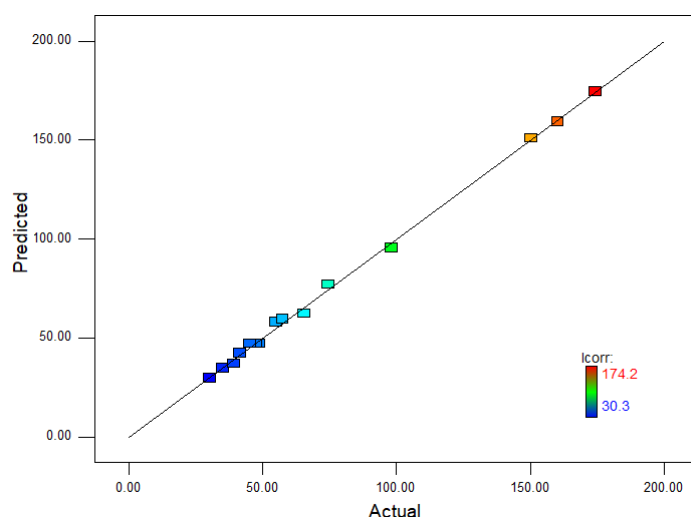


Figure 3. The predicted versus the actual data for I_{corr} model

Figure 3 shows the actual data from the experiment with the projected data provided by the model. When the points on the predicted and real graphs are near to one another and exhibit an

irregular distribution around a diagonal line, a model may be able to accurately predict experimental outcomes [37]. The points are distributed at random as seen in the plot 3, and there is good agreement between the values estimated by the model and the associated real values.

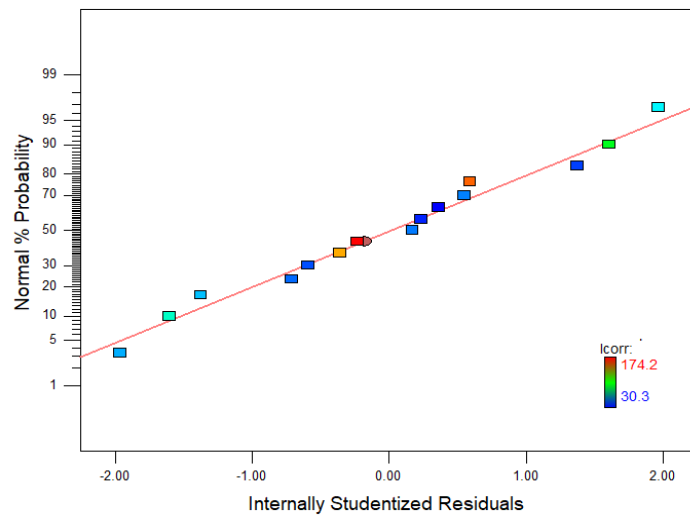


Figure 4. Normal probability versus studentized residuals for I_{corr} model

The normal plot of residuals for corrosion current density is shown in Figure 4. The graph is used to see if the discrepancy between the actual and projected outcomes follows a normal distribution [38]. The model has been shown to display a normal distribution as seen in Figure 4 because the points largely followed a diagonal straight line, demonstrating that the models fit the data correctly.

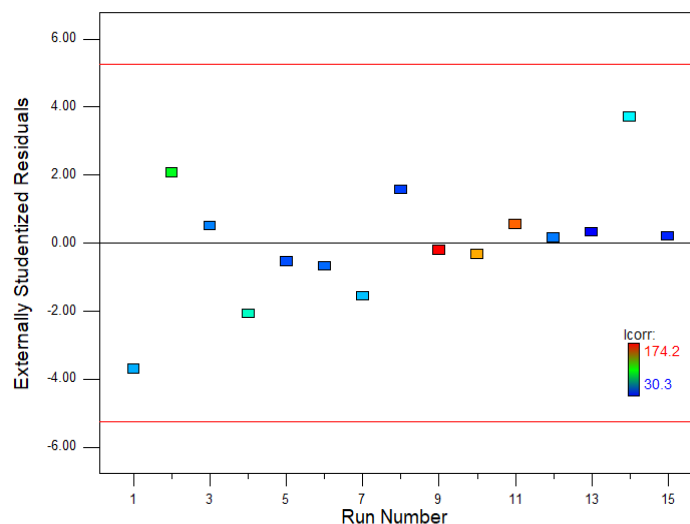


Figure 5. The externally studentized residuals versus the run order for I_{corr} model

Figure 5 shows the residuals for I_{corr} displayed against the sequence of the tests performed. This examination is done to see whether there are any hidden factors that might have affected the experiment's response. The residual points for the corrosion current density model have been spread at random across the confidence range, as shown in Figure 5. There are no data points that have surpassed the limit range, providing evidence of the absence of outliers in the residuals of model. The findings from diagnostics plots (Figures 3, 4, and 5) support the validity and suitability of the developed response models for anticipating corrosion current density.

3.5. Influence of parameters on the response (I_{corr})

The Pareto chart (Figure 6) illustrates the standardized impacts of temperature, chloride concentration, and copper concentration on the evaluation of corrosion current density in order to ascertain each factor's precise impact on (I_{corr}). The significance and size of the impacts were assessed using the Pareto chart. Each bar represents the T-value for a particular type of factor, and the bars that traverse the reference line are those that are statistically important. Thus, chloride content has the highest impact on the corrosion current density of aluminum cans. In Figure 6, all of the bars representing the factors cross the reference line at 2.57. The present model shows that these variables are statistically significant at the 0.05 level.

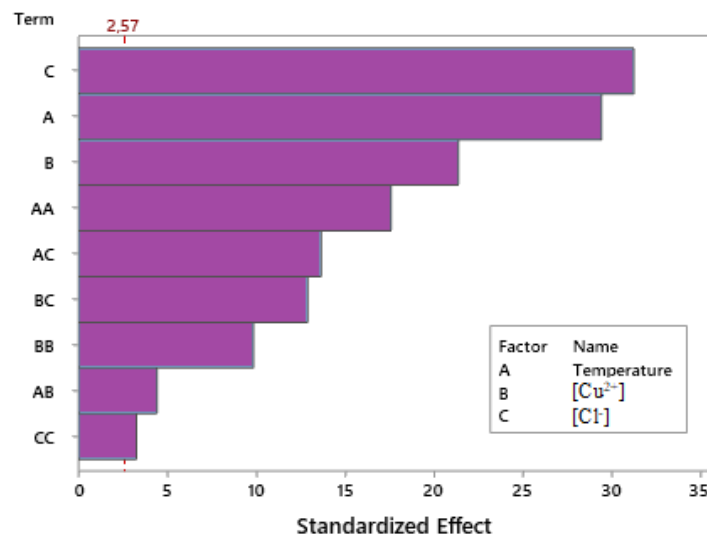


Figure 6. Pareto chart for the standardized effects of the three factors on I_{corr}

According coefficients table (Table 6), we make the conclusion that all of the study's factors have a significant influence on the corrosion current density since their p-values are less than 0.05. It has been established that all parameters under inquiry are positive, boosting the corrosion current study, consequently, the dissolution of aluminum cans. The order of the three factors' varying degrees of effect on the response value was found to be: chloride concentration > temperature > copper concentration.

Table 6. Calculated coded coefficients for corrosion current density (I_{corr})

	Coefficient	SE Coefficient	T-Value	P-Value
Constant	47.10	1.88	25.06	0.0001
T	33.88	1.15	29.44	0.0001
$[Cu^{2+}]$	24.63	1.15	21.40	0.0003
$[Cl^-]$	35.99	1.15	31.27	0.0003
T^2	29.82	1.69	17.60	0.0001
$[Cu^{2+}]^2$	16.68	1.69	9.85	0.0002
$[Cl^-]^2$	5.55	1.69	3.27	0.0221
$T^*[Cu^{2+}]$	7.23	1.63	4.44	0.0068
$T^* [Cl^-]$	22.26	1.63	13.68	0.0001
$[Cu^{2+}] * [Cl^-]$	21.00	1.63	12.90	0.0001

3.6. Representation of Model: Surface and Contour Plots

Utilizing response surface plots like 2-dimensional contour plots and 3-dimensional surface plots proves effective for establishing optimal response values and operating circumstances. A surface plot often presents a 3D image that helps to provide a better understanding of the response. On a contour plot, the response surface is viewed on a 2D plane where all points that have an equivalent response are linked to create contour lines of stable responses [55].

The 3D and contour graphs in Figure 7A show how temperature and chloride concentration affect the behavior of corrosion current density under specific circumstances. The study of this figure demonstrates that when the two parameters were increased, the corrosion current density grew from lower values (20 A/cm^2), to higher values more than (150 A/cm^2), which indicates the strength of this interaction and that both components had an equal impact on reaction. The surface response plot (Figure 7B) revealed remarkable behavior with respect to chloride and copper concentrations. Particularly, compared to $[Cl^-]$, the impact of $[Cu^{2+}]$ seemed to be steadier and more regulated. Across all levels, the effect of copper on I_{corr} remained constant. Furthermore, it became clear that the interaction of these ions had a minor impact on aluminum can corrosion.

For the combination of temperature and copper concentration, the corrosion current density seems to remain stable when $[Cu^{2+}]$ increases, we observed despite the increase in temperature

a slight increase in the corrosion rate, which implies that this interaction is the weakest compared to the others.

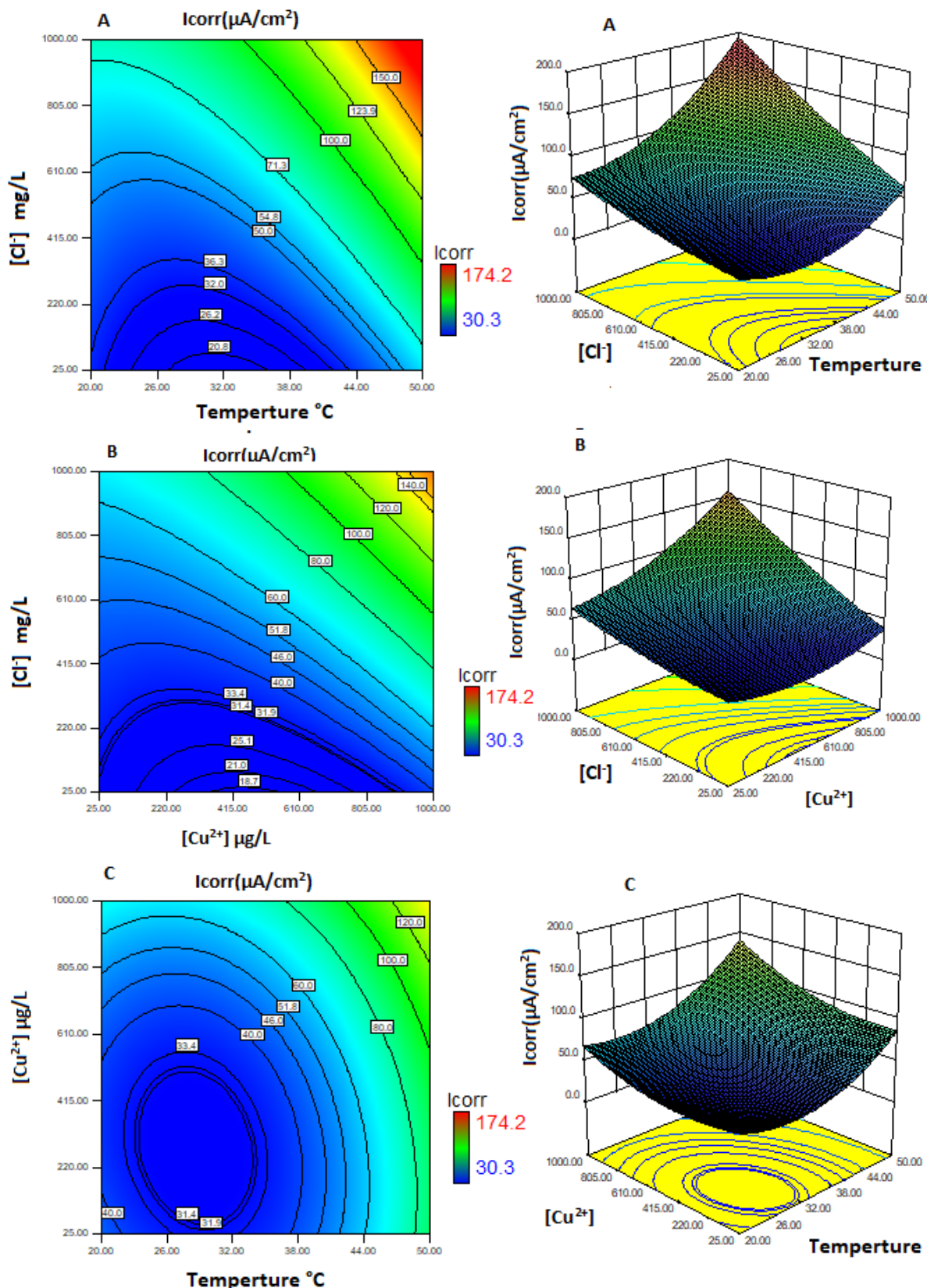


Figure 7. The influence of parameter interactions on corrosion current density

3.7. Confirmation of the developed model

The purpose of this part is to evaluate the reliability and applicability of the developed model in the food field and precisely in the beverage industry. Consequently, we assessed our model by adopting the findings of Soreas et al. as a framework. These researchers suggested a general simulation of real soft drinks using a formulation comprising citric acid pH 3.0, a chloride concentration of 250 mg/kg and a copper content of 250 g/kg [8]. Table 7 lists the factors and objectives of the prediction procedure. To achieve this goal, we executed the process utilizing the Design-Expert Software, relying on the established model for corrosion current density (I_{corr}).

Table 7. The goals of the prediction of the corrosion current density (I_{corr})

Name	Goal	Lower limit	Upper limit
Temperature (°C)	In range	20	50
[Cu ²⁺] (µg/L)	250	//	//
[Cl ⁻] (mg/L)	250	//	//
I_{corr} (µA/cm ²)	In range	30.3	174.2

Several solutions have been identified by using numerical optimization to discover the responses. It should be highlighted that the solutions were selected based on Desirability. This notion of Desirability represents a numerical value that varies from zero to one which signifying the most desirable outcome [35]. Based on the findings, a 100% Desirability was consistently observed across the entire solutions, indicating the feasibility of achieving desirable corrosion current density results under the specified conditions. The performance of our second-order model is assessed by comparing the predicted and experimental values, as shown in Table 8.

Table 8. Confirmation trials

Experience	Factors			Desirability	Response	
	Temperature (°C)	[Cu ²⁺] (µg/L)	[Cl ⁻] (mg/L)		Experiment	Prediction
1	20	250	250	1	41.28	38.695
3	42.94	250	250	1	46.7	44.929
2	50	250	250	1	76.9	74.689

The cathodic and anodic polarization curves for aluminum specimens under the various circumstances already proven are shown in Figure 8. The Tafel extrapolation method was used to acquire the values of the corrosion current density (I_{corr}), corrosion potential (E_{corr}), cathodic Tafel slope (bc), and anodic Tafel slope (ba). The outcomes are listed in Table 9.

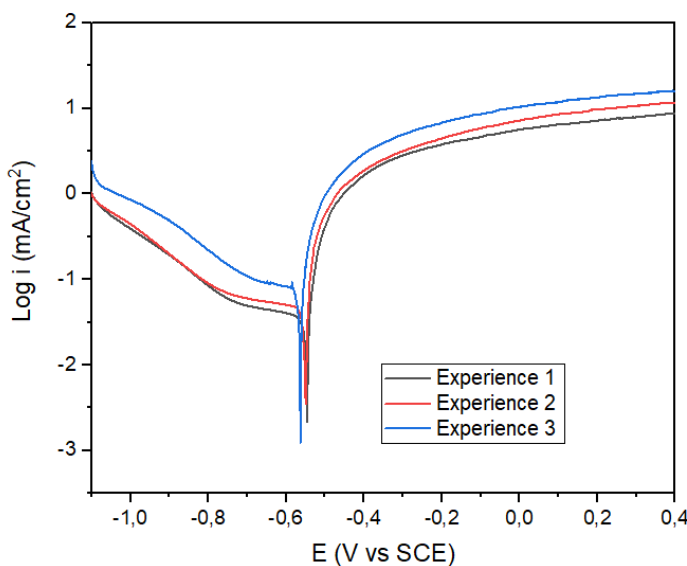


Figure 8. Potentiodynamic polarization curves recorded for aluminum under the conditions shown in Table 8

Table 9. Potentiodynamic polarization parameters for aluminum under the conditions shown in Table 8

Experiment	I_{corr}	E_{corr}	ba	$-bc$
1	76.9	-563.5	42.3	1156.7
2	46.7	-551.5	36.1	1340.5
3	37.2	-548.0	39	1353.1

It was found that the I_{corr} response is adequately connected to parameters under investigation, and that temperature is one of the factors which affects the dissolution of aluminum and therefore accelerates its corrosion. The correlation between the experimental data and the regression results showed that the proposed predictive model was highly confirmed and well accepted.

For an in-depth analysis of aluminum corrosion, we used electrochemical impedance spectroscopy, an alternative electrochemical technique that helps identify the elementary steps involved in overall corrosion processes. The appropriate Nyquist diagram, equivalent circuit, and fitting data for aluminum in citric acid with 250 mg/L of chloride and 250 g/L of copper at various temperatures are provided in Figure 9 and Table 10.

According to the findings, all Nyquist curves exhibit a single capacitive semicircle in the high-frequency (HF) area and a straight line in the low-frequency (LF) region [39]. In general, the existence of a semicircular pattern is typically linked to the charge-transfer process during the corrosion of aluminum. Contrarily, the straight line in the low-frequency area can be

attributed to Warburg impedance, which comes from either the diffusion of ions from the solution to the aluminum surface or the transportation of corrosive particles [40].

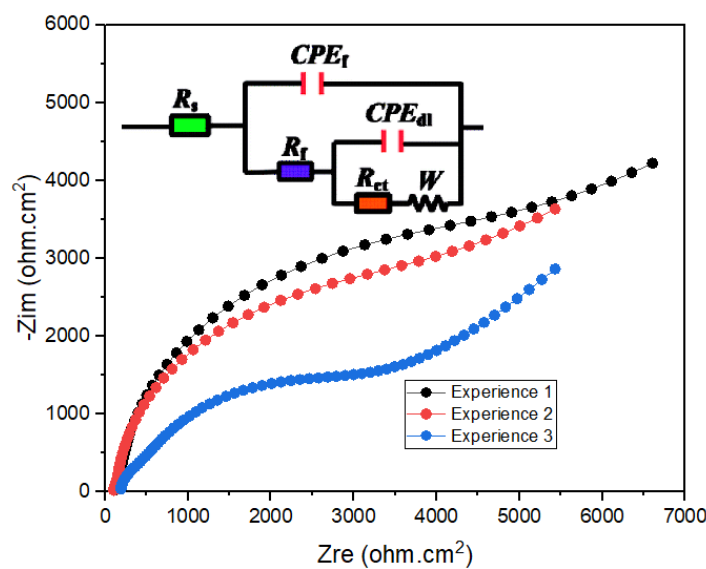


Figure 9. Nyquist plot for the aluminium electrode under the conditions mentioned in Table 8.

It is noted that when the temperature rises, the diameter of the capacitive loop decreases, suggesting the influence of this parameter on the dissolution of aluminum. The impedance outcomes in the current investigation were fitted using the equivalent circuit depicted in Figure 9. Constant phase angle elements (CPE_f and CPE_{dl}) are connected to film capacitance (C_f) and double layer capacitance (C_{dl}), respectively. In order to account for the heterogeneous nature of the electrode surface, a Constant Phase Element (CPE) is used in place of a typical capacitor [40]. The impedance parameters including solution resistance (R_s), film resistance (R_f), charge transfer resistance (R_{ct}), and Warburg impedance (W) are collected in Table 10.

Table 10. Impedance parameters for Aluminium can under the conditions listed in Table 8

Experience	R_s ($\Omega \text{ cm}^2$)	R_f ($\Omega \text{ cm}^2$)	C_f ($\mu\text{F cm}^{-2}$)	R_{ct} ($\mu\text{F cm}^{-2}$)	C_{dl} ($\mu\text{F cm}^{-2}$)	W ($\times 10^{-2} \Omega \text{ cm}^2 \text{ s}^{1/2}$)
1	177.5	562.6	5.89	4520	4.229	0.015
2	142.2	330	6.733	3800	1.474	0.011
3	154.9	367.2	7.511	2317	9.94	0.049

3.8. Surface observation

The surface morphology of the aluminum was examined before and after 6 and 24 hours of soaking in citric acid (pH 3) with 250 mg/L of chloride and 250 g/L in order to learn more

about how the aluminum can behaves in soft drinks and to support the electrochemical findings. Figure 10a depicts the sample before has been submerged in a mimetic solution where the surface is smooth with some scratches due to mechanical polishing. Figure 10c illustrates the sample after 24 hours of immersion in the acidic solution (citric acid) at 20°C, showing the existence of some pitting and spots on the aluminum surface caused by oxidation of the metal can surface. However, the surface experienced less damage and there was no evidence of corrosion products in the sample that had been submerged in the citric acid solution for six hours (Figure 10b). The outcomes supported earlier electrochemical technique findings indicating the investigated factors had an impact on the behavior of the aluminum can surface. We can also conclude that the immersion time will be a powerful and significant parameter in the corrosion of the aluminum.

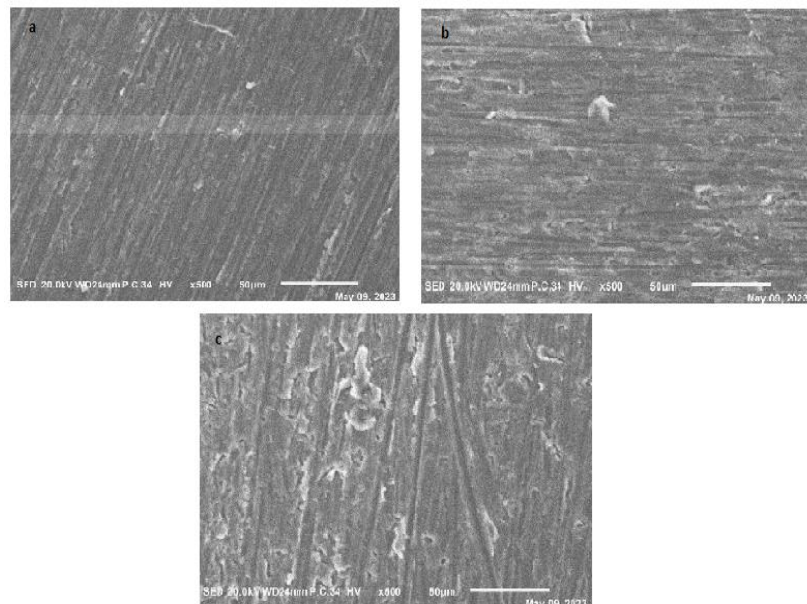


Figure 10. SEM analysis of the aluminium can under different conditions a) freshly polished b) sample immersed in the tested solution for 6h c) sample immersed in the tested solution for 24h

4. CONCLUSION

Using the statistical method Response surface methodology (RSM) with the Box-Behnken design (BBD), this study investigated the effects of temperature and the different concentrations of copper and chloride present in an aqueous solution of citric acid (pH 3), on the corrosion of aluminum cans. The potentiodynamic polarization curve was used to determine the response corrosion current density (I_{corr}). According to research findings, all of the examined independent variables had a significant and negative impact on the response, significantly enhancing the dissolution of aluminum packaging. The developed statistical model for (I_{corr}) had the greatest p-value, predicted R^2 value, and Adjusted R^2 value, indicating

that it is the best fit-model. It was shown that this equation could adequately explain the experimental data with a 95% level of confidence. Based on the electrochemical impedance spectroscopy data, the decline in both solution resistance and charge transfer resistance with increasing temperature implies an acceleration in the corrosion process. The results obtained demonstrate a notable consistency between the measurements obtained from Potentiodynamic polarization and Impedance electrochemical assessments.

Declarations of interest

The authors declare no conflict of interest in this reported work.

REFERENCES

- [1] D.S. Soares, G. Bolgar, S.T. Dantas, P.E.D. Augusto, and B.M.C. Soares, Food Packaging and Shelf Life 11 (2018) 012.
- [2] T.L. Lv, Y.Z. Rao, and Q.X. Zhang, J. Manufacturing Processes 81 (2022) 66.
- [3] S.T. Dantas, B.M.C. Soares, E.S. Saron, F.B.H. Dantas, J.A.B. Gatti, and P.H.M. Kiyataka, Packag Technol. Sci. 27 (2014) 449.
- [4] F. Riedewald, E. Wilson, and Y. Patel, Waste Management. 138 (2022) 172.
- [5] A.L.T. Martins, A.A. Couto, N.B. de. Lima, and G.F.C. Almeida, Mat. Res. 22 (2019).
- [6] A. Alankar, and M.A. Wells, Mater. Sci. Engineering. 527 (2010) 29.
- [7] K. Xhanari, and M. Finšgar, RSC Adv. 6 (2016) 62833.
- [8] B.M.C. Soares, C.A.R. Anjos, T.B. Faria, and S.T. Dantas, Packag Technol. Sci. 29 (2016) 65.
- [9] S.T. Dantas, B.M.C. Soares, E.S. Saron, F.B.H. Dantas, J.A.B. Gatti, and P.H.M. Kiyataka, Packag Technol. Sci. 27 (2014) 449.
- [10] BMC. Soares, ST. Dantas, and CAR. Anjos, J. Food Process Eng. 40 (2017).
- [11] S. Lahmady, and I. Forsal, Anal. Bioanal. Electrochem. 14 (2022) 1044.
- [12] A. Ismail, S.L. Kar, and H. Ibrahim, KEM 791 (2018) 88-94.
- [13] E. Inan-Eroglu, and A. Ayaz, J Res Med Sci. 23 (2018) 51.
- [14] T. Stahl, H. Taschan, and H. Brunn, Environ Sci Eur. 23 (2011) 37.
- [15] S.E. Kaskah, G. Ehrenhaft, J. Gollnick, and CB, Fischer. Eng. 4 (2023) 635.
- [16] Abdel-Rahman MA, Hassan SED, and El-Din MN, SN Appl Sci. 2 (2020) 573.
- [17] Z. Khoshraftar, H. Masoumi, A. Ghaemi, Case Studies in Chemical and Environmental Engineering. 7 (2023) 100329.
- [18] S.E. Kaskah, G. Ehrenhaft, J. Gollnick, and CB, Fischer. Eng. 4 (2023) 635.
- [19] N.L. Bhirud, and R.R. Gawande, IJETT. 3 (2016).
- [20] A. Permana, H. Hardi Purba, and S. Hasibuan, ComTech. 12 (2021) 99.
- [21] R. Arboretti, R. Ceccato, L. Pegoraro, and L. Salmaso, Quality & Reliability Eng. 38 (2022) 1131.

- [22] M.A. Hadiyat, B.M. Sopha, and B.S. Wibowo, Applied Sci. 12 (2022) 10663.
- [23] N.T. Chung, YS. So, W.C. Kim, and J.G. Kim, Materials. 14 (2021) 6596.
- [24] A. Nooraziah, and J. Tiagrajah, Applied Mechanics and Mater. 666 (2014) 235.
- [25] L.G. de Oliveira, AP. de Paiva, P.P. Balestrassi, J.R. Ferreira, S.C. da Costa, and P.H. da Silva Campos, Int. J. Adv. Manuf. Technol. 104 (2019) 1785.
- [26] N.K. Nguyen, J. J. Borkowski, M. Phuong Vuong, IntechOpen (2023).
- [27] B.N.G. Aliemeke, and M. OladeiNde, IJET. 6 (2020) 25.
- [28] Z. Yuan, G. Jia, and X. Cui, Fuel Processing Technology. 232 (2022) 107272.
- [29] S.S. Ranade, and P. Thiagarajan, IOP Conf Ser: Mater. Sci. Eng. 263 (2017) 022043.
- [30] S.H. Hashemi, and F. Najari, Journal of Chromatographic Sci. 57 (2019) 279.
- [31] Z. Wang, X. Han, Z. Shao, K. Xiao, Y. Fan, and S. Wang, Int. J. Electrochem. Sci. 18 (2023) 100050.
- [32] M. Šeruga, and D. Hasenay, Journal of Applied Electrochem. 31 (2001) 961.
- [33] I. Bakos, and S. Szabó, Corrosion Sci. 50 (2008) 200.
- [34] N.I. Madondo, S. Rathilal, and BF. Bakare, Catalysts. 12 (2022) 1052.
- [35] A. Khormali, and S. Ahmadi, EJ Petrol Explor Prod Technol. 15 (2023) .
- [36] G. Di Leo, and F. Sardanelli, Eur Radiol Exp. 4 (2020) 18.
- [37] P. Biniaz, M. Farsi, and MR. Rahimpour, Fuel 184 (2016) 325.
- [38] P. Kumari, and M. Lavanya, J Bio Tribol Corros. 7 (2021) 110.
- [39] O. Sisso, S. Dor, D. Eliyahu, E. Sabatani, and N. Eliaz, npj Mater Degrad. 4 (2020) 38.
- [40] Y. Qiang, S. Zhang, and Q. Xiang, RSC Adv. 8(68) (2018) 38860.